

Instrument-free quantitative gold nanoparticle-based liquid-phase colorimetric assays for use in resource-poor environments†

Received 00th January 20xx,
Accepted 00th January 20xx

Huili Wang,^a Yun Zhang,^{*a} Rongxing Li,^a Jinfang Nie,^{*a} Afaf H. El-Sagheer,^{bc} Tom Brown,^b Zhaoying Liu^a and Wencheng Xiao^a

DOI: 10.1039/x0xx00000x

www.rsc.org/

This work describes a new class of gold nanoparticle-based liquid-phase colorimetric assay (GNP-LPCA) termed as two dimensional (2D) GNP-LPCA. Its utility is demonstrated with the development of an aptamer-based 2D GNP-LPCA for simple, low-cost, sensitive, specific, and quantitative detection of adenosine as a model analyte in buffer and human serum samples with the naked eye.

Nanomaterials are materials with at least one dimension in the 1–100 nm range that have structural, electronic, optical and catalytic features significantly different from the features of bulk materials.¹ There is currently a great deal of focus on the use of various types of nanomaterials (*e.g.*, metallic and silica nanoparticles, carbon nanotubes, quantum dots, graphene, *etc.*) in the development of novel assay techniques with improved sensitivity and selectivity.² Gold nanoparticles (GNPs) have received special attentions due to their simple synthesis, high surface-to-volume ratio and absorption coefficients, and good biocompatibility.³ In particular, the unique optical property of GNPs, which is related to their surface plasmon resonance (SPR), *i.e.*, the color change in solution from red to blue during their aggregation from dispersion, has made them attractive candidates for liquid-phase colorimetric assays (LPCAs).⁴

In 1997, Mirkin pioneered the use of controllable aggregation of single-stranded DNA-coated GNPs *via* DNA hybridization for LPCA applications.⁵ Since then, the last two decades have witnessed rapid progress in the development of GNP-based LPCAs (GNP-LPCAs) for simple, sensitive and specific detection of various targets, including ions^{6a}, small molecules^{6b,c}, proteins^{6d} and DNAs.^{6e} As almost all of existing GNP-LPCAs transduce recognition chemistry into 1D (one dimensional) information (*i.e.*, the color type/intensity of the GNP solution),⁶ they can be collectively referred to as 1D GNP-LPCAs (Fig. 1A). Although the 1D GNP-LPCAs are easy to use and enable rapid

qualitative/semi-quantitative analysis by the naked eye, expensive analytical instruments such as UV-Vis spectrometers are necessary to realize quantitative detection. This adds cost and complexity to the assays and limits their applications, especially in resource-poor environments. In fact, there are so far no reports of GNP-LPCAs for economic, equipment-free quantification of analytes in solution.

In this communication, we respond to the challenge by describing a new class of GNP-LPCAs which we have named two-dimensional (2D) GNP-LPCAs. In the 2D GNP-LPCA, a GNP solution's color type/intensity is used as "first dimension" qualitative information, and the length of its blue or red colored column serves as "second dimension" information for visual quantitative analysis (Fig. 1B). In our initial proof-of-concept study, two 2D GNP-LPCAs are designed on the basis of cysteamine-mediated GNP aggregation.⁷ This model aggregation system needs no particle modification and is quite simple and rapid. Moreover, formamide is used as an "intelligent adjuster" to form a top-bottom red-blue or blue-red reaction column (Fig. 1B).⁸ This organic solvent could automatically increase the length of the blue column as the cysteamine level increases.

The analytical advantages of the 2D GNP-LPCA over traditional 1D

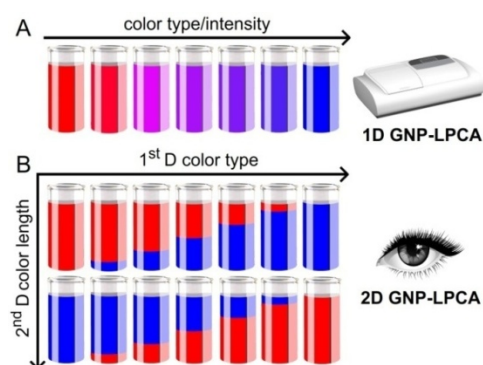


Fig. 1 Schematic analytical principles of (A) existing 1D GNP-LPCAs that rely on 1D information of the color type/intensity of a homogeneous GNP solution and use a UV-Vis spectrometer as the reader, and (B) the proposed 2D GNP-LPCAs in which a top-bottom double-color (red-blue or blue-red) column is formed and the color length constitutes the additional (secondary) dimensional information for visual quantitative analysis.

^a Guangxi Key Laboratory of Electrochemical and Magnetochemical Function Materials, College of Chemistry and Bioengineering, Guilin University of Technology, 12 Jianshan Road, Guilin 541004, China. E-mail: zy@glut.edu.cn; Niejinfang@glut.edu.cn

^b Department of Chemistry, University of Oxford, Chemistry Research Laboratory, Oxford OX1 3TA, UK

^c Chemistry Branch, Department of Science and Mathematics, Faculty of Petroleum and Mining Engineering, Suez University, Suez 43721, Egypt

† Electronic Supplementary Information (ESI) available: Experimental section and additional results. See DOI: 10.1039/x0xx00000x

GNP-LPCAs are studied in detail *via* the cysteamine detection. The second generation of (blue-red) 2D GNP-LPCA is then developed to design a new aptamer-based assay for naked-eye quantification of adenosine (model target) in buffer and human serum samples.⁹ A variety of aptamers binding various other targets that are either available or could be obtained through SELEX (systematic evolution of ligands by exponential enrichment) technique² can also be used for specific assays. The experimental section was shown in ESI†. Our results demonstrate that the new methods require only the ability to count color length-related marked bars on graduated test tubes to measure the cysteamine or adenosine levels. To our knowledge, they might be the first examples of visual quantitative 2D LPCAs where nanomaterials are adopted as colorimetric probes, thus significantly extending the concept of the 2D LPCA.⁸

Fig. 2A illustrates the working principle of the red-blue 2D GNP-LPCA based on the cysteamine-induced aggregation of unmodified GNPs prepared by a sodium citrate reduction method.¹⁰ Briefly, 30 μL of a mixture of a cysteamine sample (in buffer) and formamide ($v/v=1/1$) is added by dropwise into 100 μL of a red GNP solution. As the formamide, carrying most cysteamine with it, falls quickly during this process due to its higher density relative to water, GNP aggregation occurs at the solution's bottom *via* S-Au chemistry and zwitterionic electrostatic interactions between negatively charged GNPs and protonated cysteamine molecules.⁷ Thus, a top-bottom red-blue mixture is produced as the SPR bands of aggregated GNPs combine. The length of blue (or red) part of such dual-color solution is positively (or negatively) proportional to the cysteamine level.

The original solution of unmodified GNPs of ~ 15 nm diameter appears red in color (Fig. 2B, image 1) and displays a characteristic adsorption peak at 520 nm in the UV-Vis spectrum (Fig. 2C, curve 1). Mixing the GNP solution with the formamide caused no significant change in its color (Fig. 2B, image 2), suggesting that the GNPs were well-dispersed in formamide. Using a technique commonly used for 1D GNP-LPCA, *i.e.*, rapidly mixing a cysteamine sample in phosphate buffer solution (PBS) with a GNP solution, led to the formation of a homogeneous blue mixture (Fig. 2B, image 3; Video S1, ESI†), indicating a remarkable cysteamine-induced GNP aggregation. The aggregated particles showed a characteristic adsorption peak at 669 nm in the spectrum (Fig. 2C, curve 3). Homogeneous blue solutions were also formed by mixing GNP solutions either with a cysteamine solution in PBS *via* dropwise addition, or a cysteamine solution in both PBS and formamide ($v/v=1/1$) *via* rapid addition (Fig. 2B, images 4 and 5; Videos S2-3, ESI†).

In contrast, a top-bottom red-blue mixture solution was rapidly produced when adding 30 μL of cysteamine solution in buffer and formamide ($v/v=1/1$) into 100 μL of red GNP solution dropwise (Fig. 2B, image 6; Fig. S1, Video S4, ESI†). Its red phase displayed a UV-Vis spectrum with a clear absorption peak at 520 nm (Fig. 2C, curve 6-top), implying that the GNPs in the top of the dual-color mixture were well-dispersed. In addition, for the blue phase, while a notable decrease was found in absorption at 520 nm, a new, characteristic adsorption peak of aggregated GNPs concomitantly developed at 669 nm (Fig. 2C, curve 6-bottom). These results suggest that the use of formamide and the operating mode of dropwise addition are the two key factors to the success of the 2D GNP-LPCA.

After demonstrating the principle of the (red-blue) 2D GNP-LPCA, its analytical advantages over the 1D GNP-LPCAs were then studied.

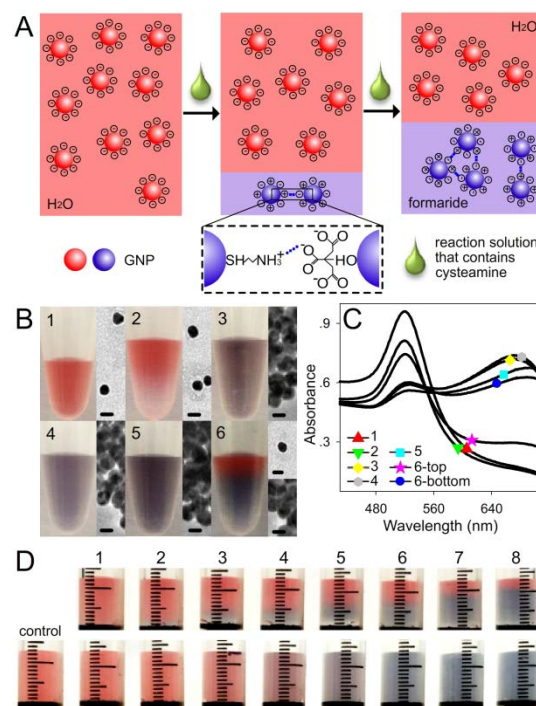


Fig. 2 (A) The working principle of red-blue 2D GNP-LPCA based on cysteamine-induced aggregation of GNPs. (B) Photographs (left) and HRTEM (high-resolution transmission electron microscopy) images (right) obtained from various solutions: 1) GNP solution; 2) dropwise addition of formamide in PBS into a GNP solution; 3) rapid mixing of 40 μM cysteamine in PBS and a GNP solution; 4) dropwise addition of 40 μM cysteamine in PBS into a GNP solution; 5) rapid mixing of 40 μM cysteamine in a mixture of PBS and formamide ($v/v=1/1$) and a GNP solution; and 6) dropwise addition of 40 μM cysteamine in a mixture of PBS and formamide into a GNP solution. Each scale bar is 15 nm. (C) Corresponding UV-Vis spectra of the solutions shown in (B). (D) Colorimetric results obtained from different cysteamine samples using (top) red-blue 2D GNP-LPCA and (bottom) 1D GNP-LPCA: 1) 0.65, 2) 1.3, 3) 2.5, 4) 5, 5) 10, 6) 20, 7) 40, and 8) 80 μM . The control is a PBS sample without the analyte.

This new 2D method was used to assay varying levels of cysteamine in PBS. Results were compared with the 1D method (Fig. 2D). For the 1D GNP-LPCA, homogeneous plasmonic reaction mixtures were obtained from all the samples (Fig. 2D, bottom). In this case, three cysteamine levels, *i.e.*, 2.5, 5 and 10 μM , can be discriminated *via* the 1D parameters of color type/intensity (Fig. 2D, bottom, images 4-6). The naked-eye limit of detection (LOD) of 1D GNP-LPCA for cysteamine was ~ 2.5 μM , where the reaction mixture remained red (Fig. 2D, bottom, image 3) but was slightly different in color from the control (Fig. 2D, bottom, image 1). A UV-Vis spectrometer can be used to optically differentiate the eight cysteamine samples tested (Fig. S2, ESI†). Their absorbance signals at 669 nm were linear over an analyte range of 0.65–5 μM (Fig. S3, ESI†).

For the 2D GNP-LPCA, all cysteamine samples led to production of different top-bottom red-blue mixtures (Fig. 2D, top, images 1-8). One can determine from image 2 in Fig. 2D (top) that the light blue color resulting from aggregated GNPs could still be observed at the bottom of the tube when the cysteamine concentration was as low as 1.3 μM . In other words, the visual LOD for the 2D GNP-LPCA was 1.3 μM as determined from the 1D color-type information. The 2D GNP-LPCA thus offers an advantage over the 1D GNP-LPCA in that the red part of each GNP solution serves as the background color reference. The color difference between the top and the bottom of

a reaction mixture can be directly used to judge the presence or absence of cysteamine in the sample without performing a control experiment. More importantly, all the red-blue solutions are clearly distinguishable using the second dimension information of lengths of their blue or red phases. That is, the length of the blue (or red) column increases (or decreases) as the target level increases. The phenomena could be attributed to the fact that the formamide allowed for a bottom-top high-low level distribution of cysteamine in the GNP solution. Thus, the longer distribution of a cysteamine level (from a higher-level sample) that can make GNPs aggregate led to the formation of a longer blue phase. As a result, counting the blue length-related marker bars on the graduated tubes in the 2D strategy (rather than using a UV-Vis spectrometer in the existing 1D methods) enabled the quantitative detection of cysteamine in a linear range from 1.3 to 80 μM (Fig. S4, ESI[†]).

Encouraged by the success of the red-blue 2D GNP-LPCA, it was further developed to design a second generation of assay. In this blue-red 2D GNP-LPCA (as depicted in Fig. 3A), the citrate-coated GNPs were first isolated from water and dispersed in formamide. Then 30 μL of a cysteamine solution in PBS was added dropwise into 100 μL of the GNP solution. Because the aqueous buffer had a lower density relative to formamide, most protonated cysteamine remained at the solution top and in turn caused the negatively charged particles to rapidly aggregate to form a top-bottom blue-red mixture (Fig. 3A). As shown in Fig. 3B, assaying cysteamine solutions in a range of 0.31–10 μM resulted in the formation of different top-bottom blue-red mixtures in which the red (or blue) column length negatively (or positively) relied on the cysteamine level. Interestingly, one can additionally discern from images 2–5 in Fig. 3B that each as-produced mixture revealed a clearer color boundary between the blue and red parts when compared with the double-color border obtained in the red-blue 2D GNP-LPCA (Fig. 2D, top). This may be due to that aggregated GNPs became increasingly larger until they sedimented at the top of red phase, thus making the blue-red boundary easier to observe by eye.

With these promising preliminary results in hand, this blue-red 2D GNP-LPCA was next adapted to design a new aptamer-based assay for visual quantitative detection of adenosine, a key cofactor in many biological processes.^{9a} It combines a superparamagnetic microparticle (SMP) platform for minimizing nonspecific adsorption effects with poly(glycidyl methacrylate) nanoparticle (PNP) and GNP probes for efficient yet robust signal amplification. The detection principle of the aptamer-based 2D GNP-LPCA is shown in Fig. 4A. In this assay, the SMP is covalently modified with short DNA strands (terminally modified with biotin) that anchor the adenosine-specific aptamer.⁹ Upon analyte addition, the aptamer binds to adenosine to form an aptamer-target complex. The biotin is then exposed for capturing the PNP (coated with streptavidin and thiol groups) onto the SMP by biotin-streptavidin reactions. The thiol groups on PNP are used to adsorb GNPs for self-assembly of numerous cysteamine *via* S-Au reactions. After magnetic separation, the analyte level, which inversely depends on the level of free cysteamine in the liquid phase, can be thus quantified by the blue-red 2D GNP-LPCA.

The feasibility and specificity of this aptamer-based 2D GNP-LPCA were evaluated by using a 10 μM cysteamine solution in PBS that could cause all the GNPs in 100 μL of formamide to fully aggregate (Fig. 3B, image 6). After the adsorption of cysteamine and magnetic

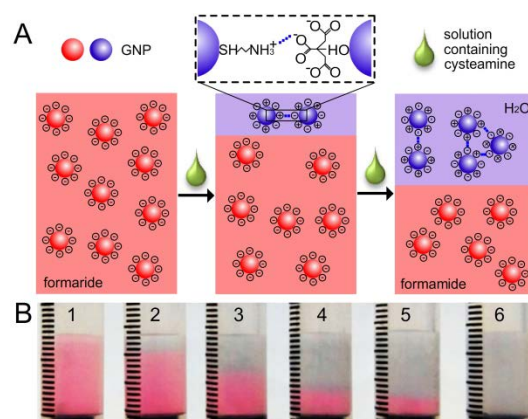


Fig. 3 (A) The working principle of blue-red 2D GNP-LPCA based on cysteamine-induced aggregation of GNPs. (B) Colorimetric results obtained from different cysteamine samples: 1) 0.31, 2) 0.62, 3) 1.25, 4) 2.5, 5) 5, and 6) 10 μM .

separation for each sample, 30 μL of the resulting supernatant was added dropwise into 100 μL of the GNP solution. As shown in Fig. 4B, in contrast to 10 μM adenosine, analysis of the control (PBS without the analyte), or 1 mM cytidine, uridine or guanosine led to formation of a homogeneous blue mixture (images 1 and 3–5). These results along with the clear blue-red solution produced from the adenosine assay (Fig. 4B, image 2) confirmed that the aptamer has excellent specificity towards its target. The aptamer-adenosine binding triggered the exposure of the biotin that captured the PNP probe, which in turn adsorbed GNPs to assemble large number of cysteamine molecules. In doing so, the low level of free cysteamine only induced the GNPs in the upper phase to aggregate.

Next, a set of buffer samples of varying adenosine levels were assayed to study analytical performance of this new method under optimized conditions (Fig. S5–S7, ESI[†]). From the results shown in Fig. 4C, one can readily distinguish the target in a level range of 9.7 nM–10 μM with naked eye. Each sample led to the formation of a unique double-color reaction mixture with a specific red column length that was negatively proportional to the analyte level (Fig. 4C). The visual LOD for adenosine which was defined as the lowest level capable of producing a top-bottom blue-red mixture was as low as 9.7 nM (Fig. 4C, image 2; Fig. S8, ESI[†]). Moreover, as shown in Fig. 4D, the aptamer-based 2D GNP-LPCA enabled equipment-free quantification of adenosine in a linear range of 9.7 nM–10 μM by visually counting marked bars in red regions of the graduated tubes. In comparison with some quantitative adenosine assays based on Raman,¹¹ fluorescence¹² or electrochemistry¹³ measurements, our method is advantageous in that it needs no external equipment to achieve comparable or better sensitivity (Table S1, ESI[†]).

To further assess its practicability, the aptamer-based 2D GNP-LPCA was used to detect adenosine in several undiluted human serum samples (Table S2, ESI[†]). The obtained recovery results are between 90.8% and 105.4% and the obtained relative standard deviation is from 7.4 to 11.1% ($n=6$). Importantly this shows that the aptamer exhibited good recognition capacity for the target even in human serum. The magnetic separation technique additionally minimized the undesirable effects of this complex matrix.

In summary, we have developed a new type of GNP-LPCA method, named 2D GNP-LPCA, which allows for the quantitative

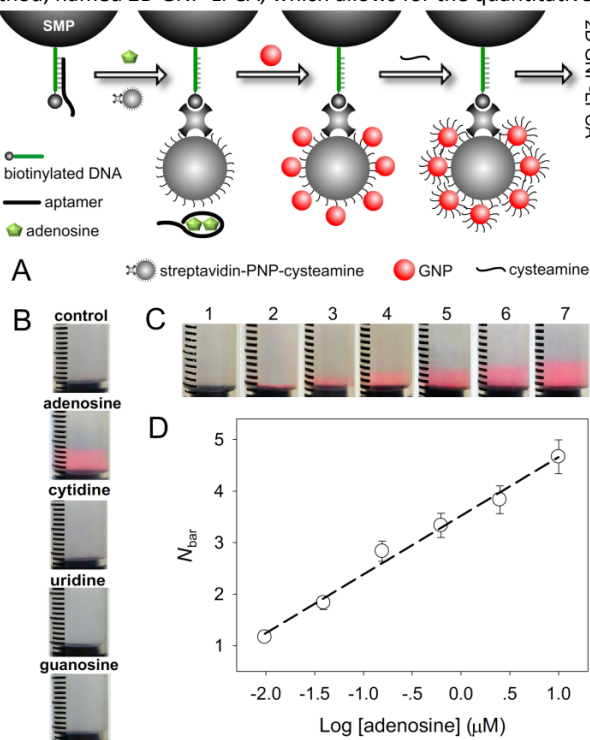


Fig. 4 (A) The working principle of aptamer-based 2D GNP-LPCA. (B) Colorimetric results obtained from different samples: the control (PBS without the analyte), 10 μM adenosine, and 1 mM cytidine, uridine and guanosine. (C) Colorimetric results obtained from different cysteamine samples: 1) 4.8 nM, 2) 9.7 nM, 3) 39 nM, 4) 0.16 μM , 5) 0.63 μM , 6) 2.5 μM and 7) 10 μM . (D) Calibration curve describing the linear relationship between number of red bars (N_{bar}) on marked test tubes shown in (C) and logarithm values of cysteamine levels (Log[cysteamine]). Its regression equation is: $y = 1.1386x + 3.5200$ ($R = 0.9948$). Each error bar represents a standard deviation across three replicate experiments.

detection of analytes without the use of a UV-Vis spectrometer. This is especially applicable for use in resource-poor settings. Moreover, it requires no additional control experiments, as the formamide-assisted color reaction has a built-in background color reference. Future work will focus on: 1) design of one-step 2D GNP-LPCAs with the sample-in-answer-out capability suitable for point-of-care applications; and 2) improvement of detection sensitivity by the development of more sensitive GNP aggregation systems.

The authors gratefully acknowledge the financial support from National Science Foundation of China (Nos. 21565012, 21365009 and 21205021), Guangxi Natural Science Foundation (Nos. 2015GXNSFFA139005 and 2014GXNSFAA118033), and Project of High Level Innovation Team/Outstanding Scholar and Key Laboratory of Food Safety and Detection in Guangxi Colleges and Universities (No. 2015GXNSFFA139005).

Notes and references

- 1 A.Q. Zhang, C.M. Lieber, *Chem. Rev.* 2016, **116**, 215.
- 2 a) P. Namdari, B. Negahdari, A. Eatemadi, *Biomed. Pharmacother.* 2017, **87**, 209; b) J.N. Tiwari, V. Vij, K.C. Kemp, K.S. Kim, *ACS Nano* 2016, **10**, 46.

- 3 a) K. Omidfar, F. Khorsand, M.D. Azizi, *Biosens. Bioelectron.* 2013, **43**, 336; b) M.S. Khan, G.D. Vishakante, H. Siddaramaiah, *Adv. Colloid Interface Sci.* 2013, **199–200**, 44; c) L.X. Yan, Z.P. Chen, Z.Y. Zhang, C.L. Qu, L.X. Chen, D.Z. Shen, *Analyst*, 2013, **138**, 4280.
- 4 a) T.T. Lou, Z.P. Chen, Y.Q. Wang, L.X. Chen, *ACS Appl. Mater. Interfaces*, 2011, **3**, 1568; b) L. Chen, J.H. Li, L.X. Chen, *ACS Appl. Mater. Interfaces*, 2014, **6**, 15897; c) Z.Y. Zhang, Z.P. Chen, S.S. Wang, C.L. Qu, L.X. Chen, *ACS Appl. Mater. Interfaces*, 2014, **6**, 6300.
- 5 R. Elghanian, J.J. Storhoff, R.C. Mucic, R.L. Letsinger, C.A. Mirkin, *Science* 1997, **277**, 1078.
- 6 a) Y. Zhou, S.X. Wang, K. Zhang, X.Y. Jiang, *Angew. Chem. Int. Ed.* 2008, **47**, 7454; b) N. Derbyshire, S.J. White, D.H.J. Bunka, L. Song, S. Stead, J. Tarbin, M. Sharman, D.J. Zhou, P.G. Stockley, *Anal. Chem.* 2012, **84**, 6 595; c) N. Fahimi-Kashani, M.R. Hormozi-Nezhad, *Anal. Chem.* 2016, **88**, 8099; d) W. Zhang, Y. Tang, J. Liu, L. Jiang, W. Huang, F.W. Huo, D.B. Tian, *J. Agric. Food Chem.* 2015, **63**, 39; e) C.C. Chang, C.P. Chen, C.Y. Chen, C.W. Lin, *Chem. Commun.* 2016, **52**, 4167.
- 7 V.V. Apyari, S.G. Dmitrienko, V.V. Arkhipova, A.G. Atmagulov, Y. A. Zolotov, *Anal. Methods* 2012, **4**, 3193.
- 8 J.F. Nie, T. Brown, Y. Zhang, *Chem. Commun.* 2016, **52**, 7454.
- 9 a) H. Liu, Y. Xiang, Y.R. Lu, M. Crooks, *Angew. Chem. Int. Ed.* 2012, **51**, 6925; b) J.W. Liu, D. Mazumdar, Y. Lu, *Angew. Chem. Int. Ed.* 2006, **45**, 7955.
- 10 N.M. Bahadur, S. Watanabe, T. Furusawa, M. Sato, F. Kurayama, I.A. Siddiquey, Y. Kobayashi, N. Suzuki, *Colloid Surf. A-Physicochem. Eng. Asp.* 2011, **392**, 137.
- 11 F.H. Ko, M.R. Tai, F.K. Liu, Y.C. Chang, *Sens. Actuat. B: Chem.* 2015, **211**, 283.
- 12 J.Q. Liu, D.G. He, Q.Q. Liu, X.X. He, K.M. Wang, X. Yang, J.F. Shangguan, J.L. Tang, Y.F. Mao, *Anal. Chem.* 2016, **88**, 11707.
- 13 D. Wu, X. Ren, L.H. Hu, D.W. Fan, Y. Zheng, Q. Wei, *Biosens. Bioelectron.* 2015, **74**, 391.